APPLICATION OF AN ALTERNATING-DIRECTION METHOD TO THE NUMERICAL SOLUTION OF THE TEMPERATURE PROBLEM FOR THE DRIVING WHEEL OF A RADIAL-INFLOW TURBINE

V. S. Petrovskii and V. I. Krichakin

UDC 536.12:621.428

A domain of complex geometry is transformed into a rectangular domain, for which the heat-conduction equations are integrated numerically by an alternating-direction method.

The immense volume of computations required in the solution of two- or three-dimensional heat-conduction problems makes it imperative to find schemes that will reduce the expenditure of machine time. This attribute is inherent in so-called efficient schemes (alternating-direction schemes) [1, 2].

Despite the considerable efficiency of these schemes, they have not been used to date for analysis of the temperature states of gas turbines. In the present article, therefore, we describe an attempt to apply an alternating-direction scheme to the numerical integration of the two-dimensional temperature problem for the driving wheel of a radial-inflow gas turbine, i.e., for an axisymmetrical body having a rather complex profile (Fig. 1). A diagram of the initial domain of integration as a simplified version of the driving-wheel cross section is given in Fig. 2.

The initial equations for the blade and the disk are, respectively,

$$\frac{\partial T_{\mathrm{b}}}{\partial \tau}=\frac{a}{\delta(r,\ z)}\left\{\frac{\partial}{\partial r}\left[\delta(r,\ z)\ \frac{\partial T_{\mathrm{b}}}{\partial r}\right]+\frac{\partial}{\partial z}\left[\delta(r,\ z)\ \frac{\partial T_{\mathrm{b}}}{\partial z}\right]\right\}-\frac{2\alpha_{\mathrm{g}}(r,\ z)_{\infty}f(\tau)}{c\rho\delta(r,\ z)}\ [T_{\mathrm{b}}-T^{*}_{\mathrm{g}}(r,\ \tau)], \quad (1)$$

$$\frac{\partial T_{\partial}}{\partial \tau}=a\left(\frac{\partial^2 T_{\partial}}{\partial r^2}+\frac{1}{r}\ \frac{\partial T_{\partial}}{\partial r}+\frac{\partial^2 T_{\partial}}{\partial z^2}\right). \quad (2)$$

Here $\tau > 0$; $f_2(z) < r \leq f_1(z)$ for the blade and $0 < r \leq f_2(r)$ for the disk; $0 \leq z \leq b_2$; $r_2 = f_2(0)$; $r_1 = f_1(0)$.

The associated boundary conditions closing the system of equations (1) and (2) are formulated in [3]. Here we discuss only the application of the alternating-direction scheme for solution of the problem.

It has been found in practice that a problem represented in finite-difference form for a curvilinear initial domain creates appreciable programming difficulties. It also increases the error of interpolation at the boundaries of the domain due to the occurrence of irregular nodes. This situation worsens the convergence of the solution.

It seems practical in this connection to replace the curvilinear domain with a rectangular domain by linear-fractional transformation. Thus, introducing new coordinates, we obtain for the disk

$$\xi=\frac{r_2}{f_2(z)}\,r,\ \eta=z, \quad (3)$$

and for the blade

$$\xi=\frac{f_2(z)-r}{f_2(z)-f_1(z)}\,(r_1-r_2+r_2),\ \eta=z.$$

Moscow Aviation Technology Institute. Translated from Inzhenerno-Fizicheskii Zhurnal, Vol. 34, No. 6, pp. 1110-1116, June, 1978. Original article submitted May 30, 1977.

0022-0841/78/3406-0753$07.50

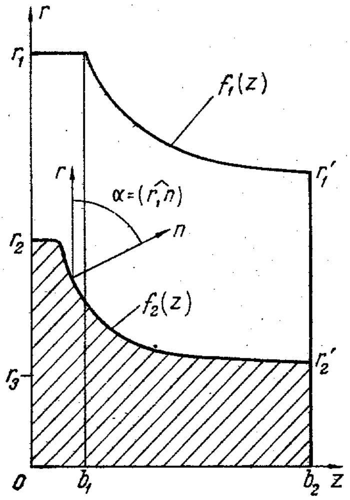

Fig. 1

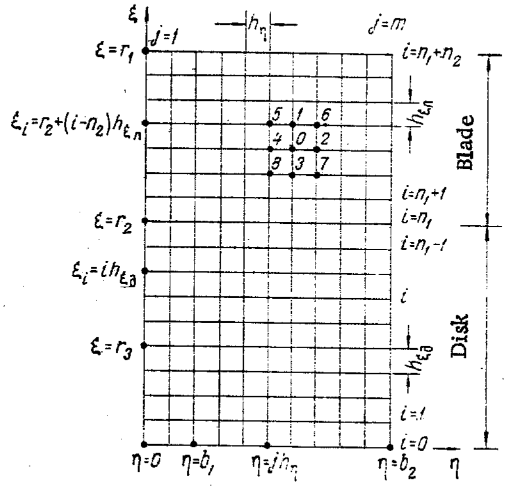

Fig. 2

Fig. 1. Schematic section of the driving wheel of a radial-inflow turbine.

Fig. 2. Computing grid for numerical solution of the temperature problem in application to the driving wheel of a radial-inflow turbine.

The initial equations (1)-(2) and the boundary conditions are transformed accordingly; for the disk

$$\frac{\partial T_\partial}{\partial \tau}=a\left[(A_\partial^2+B_\partial^2)\frac{\partial^2 T_\partial}{\partial \xi_\partial^2}+\left(A_\partial\frac{r_2}{\xi_\partial f_2(\eta)}+\frac{\partial B_\partial}{\partial \eta}\right)\frac{\partial T_\partial}{\partial \xi_\partial}+2B_\partial\frac{\partial^2 T_\partial}{\partial \xi_\partial \partial \eta}+\frac{d^2 T_\partial}{\partial \eta^2}\right], \tag{4}$$

where

$$A_\partial=\frac{r^2}{f_2(\eta)};\ B_\partial=-\frac{\xi_\partial}{f_2(\eta)}\frac{df_2(\eta)}{d\eta};$$

$$\frac{\partial B_\partial}{\partial \eta}=\frac{\xi_\partial}{[f_2(\eta)]^2}\frac{df_2(\eta)}{d\eta}-f_2(\eta)\frac{d^2 f_2(\eta)}{d\eta^2}\Big],$$

and for the blade

$$\frac{\partial T_b}{\partial \tau}=A_b\frac{\partial^2 T_b}{\partial \xi_b^2}+B_b\frac{\partial^2 T_b}{\partial \eta^2}+C_b\frac{\partial T_b}{\partial \xi_b}+D_b\frac{\partial T_b}{\partial \eta}+E_b\frac{\partial T_b}{\partial \xi_b \partial \eta}+F_b T_b+G_b, \tag{5}$$

where

$$A_b=a(\varphi_1^2+\varphi_2^2);\ B_b=a;$$

$$C_b=\frac{a}{\delta}\left(\frac{A_b}{a}\frac{\partial \delta}{\partial \xi_b}+\varphi_2\frac{\partial \delta}{\partial \eta}\right)+a\frac{\partial \varphi_2}{\partial \eta}\Big);$$

$$D_g=\frac{a}{\delta}\left(\varphi_2\frac{\partial \delta}{\partial \xi_b}+\frac{\partial \delta}{\partial \eta}\right);$$

$$E_b=2a\varphi_2;\ F_b=-\frac{2\alpha_g(\xi_b,\ \eta,\ \tau)}{c\rho\delta};\quad G=F_b T_g^*(\xi_b,\ \tau);$$

$$\delta=\delta(r,\ z)=\delta(\xi_b\eta);\ \varphi_1=\frac{r_1-r_2}{f_2(\eta)-f_2(\eta)};$$

$$\varphi_2=\frac{f_2'(\eta)(r_1-r_2)-[f_2'(\eta)-f_1'(\eta)](\xi_b-r_2)}{f_2(\eta)-f_1(\eta)}.$$

The boundary conditions take the following form in the transformed coordinate system:

$$\xi_\partial = 0; \quad \frac{\partial T_\partial}{\partial \xi_\partial} = 0; \tag{6}$$

$$\xi_{\partial(\mathrm{b})} = r_2; \tag{7}$$

$$\frac{\partial T_\partial}{\partial \xi_\partial} \frac{\cos(n,\hat{}\, z)}{f_2(\eta)} = \psi_1 \frac{\partial T_\mathrm{b}}{\partial \xi_\mathrm{b}} \frac{\cos(n,\hat{}\, r)}{f_2(\eta)} + \psi_2 T_\partial - \psi_3; \ T_\partial = T_\mathrm{b}; \tag{8}$$

$$\xi = f_1(\eta); \ 0 \leqslant \eta \leqslant b_1, \ \frac{\partial T_\mathrm{b}}{\partial \xi_\mathrm{b}} = \frac{\alpha_\mathrm{fd}(kh_\tau)}{\lambda} [T_\mathrm{g} - T_\mathrm{g}^*(r_1 kh_\tau)]; \tag{9}$$

$$b_1 < \eta \leqslant b_2, \ \frac{\partial T_\mathrm{b}}{\partial \xi_\mathrm{b}} = 0; \tag{10}$$

$$0 \leqslant \xi_\partial \leqslant r_3, \ -\frac{\partial T_\mathrm{b}}{\partial \eta} = \frac{q}{\lambda}(1 - e^{-\mu\tau}); \tag{11}$$

$$r_3 < \xi_\partial \leqslant r_2, \ -\frac{\partial T_\partial}{\partial \eta} = \frac{\alpha_\mathrm{a}(\xi)}{\lambda} [T_\partial - T_\mathrm{a}(\xi, \ kh_\tau)]; \tag{12}$$

$$r_2 < \xi_\mathrm{b} \leqslant r_1, \ \frac{\partial T_\mathrm{b}}{\partial \eta} = 0; \ \eta = b_2, \tag{13}$$

$$0 \leqslant r \leqslant r_2', \ \frac{\partial T_\partial}{\partial \xi_\partial} = 0; \tag{14}$$

$$r_2' < r \leqslant r_1', \ \frac{\partial T_\mathrm{b}}{\partial \xi_\mathrm{b}} = 0. \tag{15}$$

We describe the computing grid (Fig. 2) by families of lines $\xi_i = ih_\partial$, $i = 0, 1, \ldots, n_1$; $h_\partial = r_2/n_1$; $\xi_i = (i - n_1 - 1)h_\mathrm{b} + r_2$, $i = n_1 + 1, n_1 + 2, \ldots, n_1 + n_2 + 1$, $h_\mathrm{b} = (r_1 - r_2)/n_2$ in the domain of the disk and the domain of the blade; $\eta_j + jh_\eta$, $j = 0, 1, \ldots, m$; $h_\eta = b_2/m$. The time step is $h_\tau = T/S$, $\tau_k = kh_\tau$, $k = 0, 1, \ldots, s$; $0 < \tau \leq T$.

The finite-difference analogs of the partial derivatives are determined on a nine-point mask.

We first write the difference equations and boundary conditions in explicit form with respect to η and in implicit form with respect to ξ. Then the partial derivatives with respect to η are found in terms of the known temperature of the k-th layer, and the partial derivatives with respect to ξ are written to include the unknown temperature of the $(k + \frac{1}{2})$-th layer.

For the domain of the disk $(0 < i < n_1)$

$$\frac{T_i^{k+1/2} - T_{s_0}^k}{0.5\,h_\tau} = a\Big[(A_\partial^2 + B_\partial^2)_{s_0} \frac{T_{i-1}^{k+1/2} - 2T_i^{k+1/2} + T_{i+1}^{k+1/2}}{h_\xi^2} + \left(\frac{A_\partial r_2}{\xi_\partial f_2} + \frac{\partial B_\partial}{\partial \eta}\right) \frac{T_{i+1}^{k+1/2} - T_{i-1}^{k+1/2}}{2h_\xi} + 2B_{\partial,s_0} \times \frac{T_{s_6}^k - T_{s_7}^k + T_{s_8}^k - T_{s_5}^k}{4h_\xi h_\eta} + \frac{T_{s_4}^k - 2T_{s_0}^k + T_{s_2}^k}{h_\eta^2}\Big]. \tag{16}$$

For the domain of the blade $(n_1 + 1 < i < n_1 + n_2 + 1)$

$$\frac{T_i^{k+1/2} - T_i^k}{0.5h_\tau} = A_{\mathrm{b},s_0} \frac{T_{i-1}^{k+1/2} - 2T_i^{k+1/2} + T_{i+1}^{k+1/2}}{h_\xi^2} +$$

$$+B_{b s_0}\frac{T^k_{s_4}-2T^k_{s_0}+T^k_{s_2}}{h^2_\eta}+C_{b,s_0}\frac{T^{k+1/2}_{i+1}-T^{k+1/2}_{i-1}}{2h_\xi}+D_{b s_0}\frac{T^k_{s_2}-T^k_{s_4}}{2h_\eta}+$$

$$+E_{b,s_0}\frac{T^k_{s_6}-T^k_{s_5}+T^k_{s_6}-T_{s_7}}{4h_\xi h_\eta}+F_{b,s_0}T^{k+1/2}_i+G_{b,s_0}. \tag{17}$$

The boundary conditions for the first state of the computations are

$$\xi_\partial=0\ (i=0),\ T^{0,k+1/2}=T^{1,k+1/2}; \tag{18}$$

$$\xi=r_2\ (i=n_1\ \text{or}\ i=n_1+1);$$

$$\frac{T^{k+1/2}_{n_1}-T^{k+1/2}_{n_1-1}}{h_\xi}\ \frac{\cos(n,\hat{}\,z)}{f_2(\eta)}=\psi_1\frac{T^{k+1/2}_{n_1+2}-T^{k+1/2}_{n_1}}{h_\xi}+ \tag{19}$$

$$+\psi_2T^{k+1/2}_{n_1}-\psi_3; \tag{19}$$

and

$$T^{k+1/2}_{n_1}=T^{k+1/2}_{n_1+1};\ \xi_b=r_1\ (i=n_1+n_2+1); \tag{20}$$

$$\frac{T^{k+1/2}_{n_1+n_2+1}-T^{k+1/2}_{n_1+n_2}}{h_\xi}=\frac{\alpha_{fd}(kh_\tau)}{\lambda}[T^*_g(r_1,\ kh_\tau)-T^{k+1/2}_{n_1+n_2+1}]. \tag{21}$$

The systems of grid equations for integration by columns ($j = 1, 2, \ldots, m-1$) are tridiagonal, i.e.,

$$A_iT^{k+1/2}_{i-1}-B_iT^{k+1/2}_i+C_iT^{k+1/2}_{i+1}=-F^k_i$$
$$(i=1,\ 2,\ldots,\ n_1+n_2). \tag{22}$$

The constants A_i, B_i, C_i and the function F_i are determined from (16) and (17).

The boundary conditions for the columns for $i = 0$ and $i = n_1 + n_2 + 1$ are written in the form

$$T^{k+1/2}_0=\chi_1T^{k+1/2}_1+\nu_1,\ i=0,$$

where $\chi_1 = 1$ and $\nu_1 = 0$;

$$T^{k+1/2}_{n_1+n_2+1}=\chi_2T^{k+1/2}_{n_1+n_2}+\nu_2,\ i=n_1+n_2+1.$$

Here for $\eta = b_1$

$$\chi_2=\frac{\lambda}{\lambda+\alpha_{fd}(kh_\tau)h_\xi};\quad \nu_2=\frac{\alpha_{fd}(kh_\tau)T^*_g(r_1,\ kh_\tau)h_\xi}{\lambda+\alpha_{fd}(kh_\tau)h_\xi},$$

and for $\eta \leq b_1$ we have $\chi_2 = 1$ and $\nu_2 = 0$. From the recursion formulas

$$\alpha_{i+1}=\frac{C_i}{B_i-\alpha_iA_i};\qquad \beta_{i+1}=\frac{\beta_iA_i+F^k_i}{B_i-\alpha_iA_i}, \tag{23}$$

in which $\alpha_1 = \chi_1$ and $\beta_1 = \nu_1$, we determine α_i and β_i ($i = 1, 2, \ldots, n_1 + n_2$). The computation advances from bottom to top. We then find

$$T^{k+1/2}_{n_1+n_2+1}=\frac{\nu_2+\chi_2\beta_{n_1+n_2+1}}{1-\chi_2\alpha_{n_1+n_2+1}}. \tag{24}$$

Finally, we determined

$$T^{k+1/2}_i=\alpha_{i+1}T^{k+1/2}_{i+1}+\beta_{i+1},\ i=0,\ 1,\ldots,\ n_1+n_2. \tag{25}$$

The computation advances from top to bottom. The temperature is found for all $j = 1, 2, \ldots, m-1$.

This completes the first pass of the computations of the temperature in the $(k + \frac{1}{2})$-th layer in terms of the known temperature in the k-th layer.

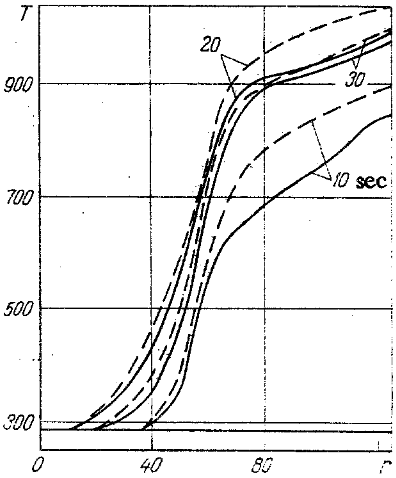

Fig. 3

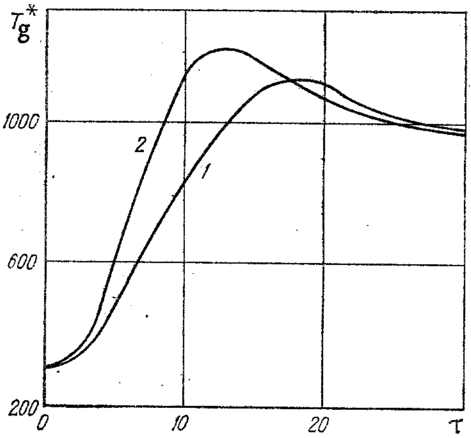

Fig. 4

Fig. 3. Results of numerical solution of the temperature problem for $z = 10^{-2}$ m (Fig. 1). The solid curves are plotted for the function $T_g^*(\tau)$ represented by curve 1 in Fig. 4; r in $m \cdot 10^{-3}$.

Fig. 4. Temperature T_g^*, °K, versus time τ, sec, taken as initial functions for solution of the temperature problem.

In the next pass of the computations the initial difference equations are written in explicit and implicit form with respect to ξ and η, respectively. The partial derivatives with respect to ξ are now found directly in terms of the known temperature of the $(k + \frac{1}{2})$-th layer, while those with respect to η are written to include the temperature of the $(k + 1)$-th layer.

The grid equations for the second stage take the form

$$A_j T_{j-1}^{k+1} - B_j T_j^{k+1} + C_j T_{j+1}^{k+1} = -F_j^{0,k+1/2}. \tag{26}$$

The coefficients A_j, B_j, C_j and the function $F_j^{0,k+1/2}$ are also determined from Eqs. (16) and (17), but with the latter written to take account of the transition from the $(k + \frac{1}{2})$-th to the k-th layer in a somewhat different form.

The boundary conditions for the rows are written in the following form:

$$\text{for} \quad j = 0 \quad T_0^{k+1} = \chi_1 T_1^{k+1} + \nu_1. \tag{27}$$

For $\xi_\partial < r_3$

$$\chi_1 = 1, \quad \nu_1 = -\frac{h_\eta q(1 - e^{-\mu\tau})}{\lambda};$$

For $\xi_\partial \geq r_3$

$$\chi_1 = \frac{\lambda}{\lambda + \alpha_a(ih_{\xi\partial})h_\eta}; \quad \nu_1 = \frac{\alpha_a T_a h_\eta}{\lambda + \alpha_a h_\eta};$$

for j = m

$$T_m^{k+1/2} = \chi_2 T_{m-1}^{k+1} + \nu_2. \tag{28}$$

Here $\chi_2 = 1$ and $\nu_2 = 0$.

From the recursion formulas

$$\alpha_{j+1} = \frac{C_j}{B_j - \alpha_j A_j}, \quad \beta_{j+1} = \frac{A_j B_j + F_j^{k+1/2}}{B_j - \alpha_j A_j}, \tag{29}$$

in which $\alpha_1 = \chi_1$ and $\beta_1 = \nu_1$, we determine α_j and β_j $(j = 1, 2, \ldots, m - 1)$. The computation advances from left to right. We then find

$$T_m^{k+1} = \frac{\nu_2 + \chi_2\beta_m}{1 - \chi_2\alpha_m}. \tag{30}$$

Next we determine

$$T_j^{k+1} = \alpha_{j+1}T_{j+1}^{k+1} + \beta_{j+1}. \tag{31}$$

The computation advances from right to left.

The temperature in row $i = n_1$ is found in terms of the temperature in rows $n_1 - 1$ and $n_2 + 2$:

$$T_{n_1,j}^{k+1} = \left(\frac{T_{n_1-1,j}^{k+1}}{h_\xi} + \psi_1 \frac{T_{n_1+2,j}^{k+1}}{h_\xi} + \psi_3\right)\left(\frac{1}{h_\xi} + \frac{\psi_1}{h_\xi} - \psi_2\right)^{-1}. \tag{32}$$

This completes the second pass of the computation of the temperature in the (k + 1)-th layer. The transition from the (k + 1)-th to the (k + 2)-th layer is analogous.

Thus, in the proposed efficient scheme the initial two-dimensional problem is partitioned into two one-dimensional problems, one of which is solved with the use of an explicit scheme, and the other with an implicit scheme. This approach optimally combines the advantages of both schemes. For the implicit scheme the number of operations is $O(1/h_\xi h_\eta)$, which is lower by two orders with respect to h_ξ and h_η than the number of operations in the implicit scheme: $O(1/h_\xi^2 h_\eta^2)$. However, the choice of h_τ for the explicit scheme is limited by the stability condition $h_\tau \leq h_\xi h_\eta/4$, whereas the implicit scheme is unconditionally stable for any h_ξ and h_η.

The results of a computation by the proposed method are given, as an example, in Fig. 3. The object of the computations is the driving wheel of the turbine of an aircraft booster engine. The temperature dependences are found for two different time variations of T_g^* (Fig. 4) at $z = 10^{-2}$ m, i.e., in the cross section coinciding with the maximum blade height. It is seen that the steeper rise of T_g^* in the blade zone (curve 2 in Fig. 4) increases the heating rate (dashed curves in Fig. 3).

LITERATURE CITED

1. A. N. Tikhonov and A. A. Samarskii, Equations of Mathematical Physics [in Russian], Nauka, Moscow (1966).
2. R. Bellman and E. Angel, Dynamic Programming and Partial Differential Equations, Academic Press, New York (1972).
3. V. S. Petrovskii and E. E. Denisov, Inzh.-Fiz. Zh., 22, No. 5 (1974).
4. V. S. Petrovskii and A. M. Polyakov, Aviats. Tekh., No. 4 (1973).